

^{14}N NQR and relaxation at the ferroelectric transition in NaNO_2

R. Ambrosetti, R. Angelone, and A. Colligiani

Laboratorio di Chimica Quantistica ed Energetica Molecolare del Consiglio Nazionale delle Ricerche, I56100 Pisa, Italy

A. Rigamonti

Istituto di Fisica dell'Università, I27100 Pavia, Italy

and Gruppo Nazionale di Struttura della Materia del Consiglio Nazionale delle Ricerche, Unità di Pavia, Italy

(Received 18 October 1976)

^{14}N nuclear quadrupole resonance and relaxation measurements in NaNO_2 around the ferroelectric transitions have been performed by pulse and Fourier-transform technique, with high-temperature resolution and accuracy. In the narrow temperature range in which the antiferroelectric phase exists and where previous authors failed to detect the nuclear-quadrupole-resonance (NQR) signals, the splitting of the ν_+ and ν_- lines in two components were observed. A theory is developed to connect the NQR parameters to the torsional vibrations of the NO_2^- ions as well as to the order-disorder reorientational fluctuations driving the transitions. The critical fluctuations are described through a kinematical Ising model. It is proven that the reorientational order-disorder variable is reversed by an angle which is not exactly π . By analyzing the experimental results in the light of the theoretical treatment interesting information on the critical dynamics is obtained.

I. INTRODUCTION

Sodium nitrite is an interesting ferroelectric crystal. Besides its structural simplicity, the relevance of NaNO_2 stands on the features of the critical dynamics driving the phase transitions. In the paraelectric phase the NO_2^- dipoles are subjected to reorientational fluctuations along the \vec{b} axis; it is quite established¹ that the flipping between the two equilibrium sites involves a sudden rotation of NO_2^- around the \vec{c} axis (O-O direction). The transition to the ferroelectric phase is of order-disorder type, with small lattice displacements occurring at $T_c \approx 164^\circ\text{C}$. In a narrow temperature range above T_c an antiferroelectric phase exists, with the NO_2^- dipoles "sinusoidally" distributed along the \vec{a} axis with a period of few lattice cells.¹

Accurate dielectric measurements²⁻⁴ have been explained on the basis of a dynamical Ising model, the dichotomic variable being the orientation of the NO_2^- dipole. No strongly temperature dependent soft modes were found by means of various infrared and Raman spectroscopy experiments. Neutron inelastic scattering⁵ showed, in the paraelectric phase, a quasielastic component, related to the ferroelectric fluctuations. Therefore the critical dynamics in NaNO_2 can be considered as superimposed on the ordinary phonon dynamics and causing a relaxational-type central component in the spectrum of the collective excitations. The existence of this central peak can be discussed along the lines recently pointed out by Barker.⁶ It could also be related, according to Beck,⁷ to the dynamics of double-well coupled anharmonic oscillators.

An excellent tool to investigate the critical dynamics in NaNO_2 is offered by the quadrupole resonance and relaxation of the ^{14}N nucleus. Indeed, various authors⁸⁻¹¹ have performed ^{14}N nuclear-quadrupole-resonance (NQR) measurements. However, no sizeable signal around the transition and in the paraelectric phase have been detected. Recently Petersen and Bray¹² were able to extend the NQR measurements up to 194°C . The temperature range around the antiferro- and ferroelectric transition, however, was not explored with high-temperature resolution and the results were not analyzed in the light of the critical dynamics.

In this paper we report accurate ^{14}N NQR measurements in NaNO_2 , performed by means of high-resolution pulse technique and with a temperature resolution better than 0.1° , around the transition temperatures. In particular, in the antiferroelectric phase we were able to put in evidence the splitting of the ν_+ and ν_- lines in two components. The NQR parameters have been theoretically related to the critical dynamics of the NO_2^- dipoles and interesting information is deduced. In Sec. II the theory for a meaningful interpretation of the data is developed. In Sec. III the experimental results are presented. Finally (Sec. IV), the data are analyzed and discussed and the main conclusions are emphasized.

II. THEORY

The motions of the NO_2^- groups around the transitions are fast compared to the inverse NQR frequencies. Therefore, the resonance frequencies, the linewidths, and the relaxation rates can

be derived by writing,¹³ for the electric field gradient (EFG) components,

$$\begin{aligned} V_{jk}(t) &= \langle V_{jk} \rangle + V_{jk}(t) - \langle V_{jk} \rangle \\ &= \langle V_{jk} \rangle + V_{jk}^f(t). \end{aligned} \quad (1)$$

The time-averaged components $\langle V_{jk} \rangle$ give the resonance frequencies. The fluctuating parts $V_{jk}^f(t)$ cause line broadening and drive the nuclear relaxation. V_{jk} in Eq. (1) are the EFG components in the polarization laboratory frame xyz , with $\vec{x} = \vec{c}$, $\vec{y} = \vec{a}$, and $\vec{z} = \vec{b}$. These axes coincide with the principal axes XYZ of the ¹⁴N EFG tensor when the NO₂⁻ group is in the equilibrium position.¹⁴

The asymmetry parameter $\eta = (V_{xx} - V_{yy})/V_{zz}$ is not zero. Therefore, one has the eigenstates $|+\rangle$, $|-\rangle$, and $|0\rangle$ of the quadrupole Hamiltonian, with the resonance frequencies ν_+ , ν_- , and ν_d [$\nu_{\pm} = (E_{\pm} - E_0)/h$, $\nu_d = (E_+ - E_-)/h$] and the relaxation transition probabilities W_+ , W_- , and W_d . These can be related to the $V_{jk}^f(t)$ in Eq. (1) through the usual application of the time-dependent perturbation theory. The appropriate spectral densities at $\omega_{\pm, d}$ of the correlation functions for the matrix elements of the quadrupole Hamiltonian¹³ connecting the $|+\rangle$, $|-\rangle$, and $|0\rangle$ eigenstates are involved. By expressing these eigenstates in terms of those for I_z one finally obtains

$$W_+ = A \int e^{-i\omega_+ t} \langle V_{yz}(0) V_{yz}(t) \rangle dt, \quad (2a)$$

$$W_- = A \int e^{-i\omega_- t} \langle V_{xz}(0) V_{xz}(t) \rangle dt, \quad (2b)$$

$$W_d = A \int e^{-i\omega_d t} \langle V_{xy}(0) V_{xy}(t) \rangle dt, \quad (2c)$$

where $A = e^2 Q^2 / 4\hbar^2$ (the index f will be omitted).

The EFG at the ¹⁴N site can be considered as the sum of two contributions: a *local* contribution due to the electronic and nuclear charges of the NO₂⁻ group under consideration and an *external* contribution due to all other charges (Na⁺ and NO₂⁻). As motions providing the temperature dependence of the NQR parameters we will consider the following: (i) for the local contribution, the sudden rotations of the NO₂⁻ around the \vec{c} axis as well as the torsional vibrations about the \vec{a} , \vec{b} , and \vec{c} axes; (ii) for the external contribution, the effective modulation of the EFG at ¹⁴N arising from the reorientation of the NO₂⁻ under consideration. The effects due to other motions of Na⁺ and NO₂⁻ can be neglected around the transitions, in view of the high frequency involved and the smallness of the external contribution compared to the local one.¹⁴

A. Time dependence of the local EFG

Let φ_a , φ_b , and φ_c indicate the angles of the torsional vibrations around an equilibrium site.

The critical reversing of the NO₂⁻ group will be described by a kinematical Ising model,¹⁵ which was proved fruitful in the interpretation of the dielectric measurements in NaNO₂.^{2,3} Therefore the angle α between the \vec{Z} EFG principal axis and the $\vec{z} = \vec{b}$ axis will be written

$$\alpha(t) = \frac{1}{2} (\pi + \varphi^*) - \frac{1}{2} (\pi + \varphi^*) s(t) + \varphi_c(t), \quad (3)$$

where $s(t)$ is a local order-disorder variable which assumes the values $+1$ and -1 . φ^* is a random variable which allows reversal of an angle which is not exactly π . The inclusion of φ^* generalizes the classical Ising model⁹ ($\varphi^* = 0$) and it is supported by the following physical argument. The NO₂⁻ group executes flipping transitions in a double well potential and oscillations in a well of finite width. Therefore the reversing occurs by angles which differ, in general, from π by a quantity of the order of φ_c . It should be stressed that $\varphi^* \neq 0$ is required by the experimental results (for $\varphi^* = 0$ no NQR parameter would be affected by the transition, in contrast with the experimental evidence, as it will be pointed out later on).

While φ^* takes different values at the various jumps of $s(t)$ one should have

$$\langle \varphi^{*2} \rangle = \alpha \langle \varphi_c^2 \rangle, \quad (4)$$

α being a constant of the order of unity.

The instantaneous $V_{jk}(t)$ can be obtained in terms of the EFG components V_{JK} in the principal-axes frame of reference by the usual tensor transformations involving φ_a , φ_b , and α . One obtains

$$\begin{aligned} V_{xx}(t) &= (1 - \varphi_a^2 - \varphi_b^2) V_{XX} + \varphi_b^2 V_{YY} + \varphi_a^2 V_{ZZ}, \\ V_{yy}(t) &= (\varphi_a \sin \alpha + \varphi_b \cos \alpha)^2 V_{XX} \\ &\quad + [(1 - \varphi_b^2) \cos^2 \alpha \\ &\quad - 2\varphi_a \varphi_b \sin \alpha \cos \alpha] V_{YY} \\ &\quad + [(1 - \varphi_a^2) \sin^2 \alpha] V_{ZZ}, \\ V_{zz}(t) &= (\varphi_a \cos \alpha - \varphi_b \sin \alpha)^2 V_{XX} \\ &\quad + [(1 - \varphi_b^2) \sin^2 \alpha \\ &\quad + 2\varphi_a \varphi_b \sin \alpha \cos \alpha] V_{YY} \\ &\quad + (1 - \varphi_a^2) \cos^2 \alpha V_{ZZ}, \\ V_{xz} &= (\varphi_a \cos \alpha - \varphi_b \sin \alpha) V_{XX} \\ &\quad + \varphi_b \sin \alpha V_{YY} - \varphi_a \cos \alpha V_{ZZ}, \\ V_{xy} &= (-\varphi_a \sin \alpha - \varphi_b \cos \alpha) V_{XX} \\ &\quad + \varphi_b \cos \alpha V_{YY} + \varphi_a \sin \alpha V_{ZZ}, \\ V_{yz} &= \cos \alpha \sin \alpha (V_{YY} - V_{ZZ}). \end{aligned} \quad (5)$$

By taking into account Eq. (3) the time-averaged components result in

$$\begin{aligned}\langle V_{xx} \rangle &= (1 - \langle \varphi_a^2 \rangle - \langle \varphi_b^2 \rangle) V_{XX} + \langle \varphi_b^2 \rangle V_{YY} + \langle \varphi_a^2 \rangle V_{ZZ}, \\ \langle V_{yy} \rangle &= \langle \varphi_b^2 \rangle V_{XX} + (1 - \langle \varphi_b^2 \rangle - \langle \varphi_c^2 \rangle - \chi) V_{YY} \\ &\quad + (\varphi_c^2 + \chi) V_{ZZ}, \\ \langle V_{zz} \rangle &= \langle \varphi_a^2 \rangle V_{XX} + (\langle \varphi_c^2 \rangle + \chi) V_{YY} \\ &\quad + (1 - \langle \varphi_a^2 \rangle - \langle \varphi_c^2 \rangle - \chi) V_{ZZ},\end{aligned}\quad (6)$$

where

$$\chi = (1 - \langle s \rangle)^{\frac{1}{2}} \langle \varphi^{*2} \rangle, \quad (7)$$

while $\langle V_{jk} \rangle = 0$ for $j \neq k$. The fluctuating components can be written in the form

$$\begin{aligned}V_{xy}(t) &= \varphi_b s(t) (V_{YY} - V_{XX}), \\ V_{xz}(t) &= \varphi_a s(t) (V_{XX} - V_{ZZ}), \\ V_{yz}(t) &= [\varphi_c + f(t)] (V_{YY} - V_{ZZ}),\end{aligned}\quad (8)$$

where

$$f(t) = [1 - s(t)]^{\frac{1}{2}} \varphi^*. \quad (9)$$

The diagonal fluctuating components do not present first order contributions in φ and therefore can be neglected.

B. Time dependence of the external EFG

For the external contribution one can distinguish between that which arises from the Na^+ ions and that from the other NO_2^- groups. Regarding the first one, the EFG at the i th nucleus can be written

$$V_{jk}^{(i)}(t) = S_{jk} + A_{jk} s_i(t), \quad (10)$$

where $s_i(t)$ is the order-disorder variable and S and A are the symmetric and antisymmetric part of V_{jk} , i.e.,

$$S_{jk} = \frac{1}{2} [V_{jk}(+) + V_{jk}(-)], \quad (11a)$$

$$A_{jk} = \frac{1}{2} [V_{jk}(+) - V_{jk}(-)]. \quad (11b)$$

$V_{jk}(\pm)$ means the EFG at the ^{14}N site when the NO_2^- taken in to reference is at the + or - position, respectively. Owing to the high symmetry of the NaNO_2 crystal one has

$$A_{jk} = 0, \quad S_{jk} = V_{jk}(+), \quad (12)$$

i.e., the contribution from Na^+ does not involve the critical dynamics.

For the EFG from the NO_2^- 's, we write

$$\begin{aligned}V_{jk}^{(i)}(t) &= \sum_I B_{jk}^{(i,I)} + C_{jk}^{(i,I)} s_i(t) \\ &\quad + D_{jk}^{(i,I)} s_i(t) + E_{jk}^{(i,I)} s_i(t) s_i(t),\end{aligned}\quad (13)$$

where B , C , D , and E can easily be expressed in terms of $V_{jk}^{(i,I)}(\pm, \pm)$. By taking into account, in Eq. (13), the symmetry properties one obtains

$$\langle V_{jk} \rangle = \sum_I B_{jk}^{(i,I)}, \quad (14)$$

while for the fluctuating components

$$V_{jk}(t) = \sum_I D_{jk}^{(i,I)} s_i(t). \quad (15)$$

In Eq. (14) $B_{jk}^{(i,I)}$ stands for

$$B_{jk}^{(i,I)} = \frac{1}{2} [V_{jk}^{(i,I)}(++) + V_{jk}^{(i,I)}(--)], \quad (16)$$

and only monopole terms contribute to it [since for the dipole contribution $V_{jk}^{(i,I)}(\pm, +) = -V_{jk}^{(i,I)}(\pm, -)$]. $D_{jk}^{(i,I)}$ in Eq. (15) stands for

$$\begin{aligned}D_{jk}^{(i,I)} &= \frac{1}{4} [V_{jk}^{(i,I)}(++) - V_{jk}^{(i,I)}(+-) \\ &\quad + V_{jk}^{(i,I)}(-+) - V_{jk}^{(i,I)}(--)],\end{aligned}\quad (17)$$

and both monopole and dipole terms contribute to it. It must be stressed that

$$\sum_I D_{jk}^{(i,I)} = 0. \quad (18)$$

C. Conclusive expressions of the NQR parameters

According to Eqs. (10) and (12) for Na^+ 's and Eqs. (14) and (16) for NO_2^- 's, the external contributions to $\langle V_{jk} \rangle$ do not involve the critical dynamics. Moreover, these "rigid lattice" contributions should be small compared to the local one (around a few percent according a point charge evaluation¹⁴). Therefore, we will derive the temperature dependence of the static quadrupole coupling around the transitions by taking into account only Eqs. (6). According to the standard notation we can write

$$\begin{aligned}e^2 Qq/h &= (e^2 Qq_0/h) \\ &\quad \times [1 - \frac{1}{2}(3 + \eta_0)(\langle \varphi_c^2 \rangle + \chi) - \frac{1}{2}(3 - \eta_0)\langle \varphi_a^2 \rangle]\end{aligned}\quad (19)$$

and

$$\begin{aligned}\eta &= \eta_0 [1 - 2\langle \varphi_b^2 \rangle + \frac{1}{2}(3 - \eta_0)(1 + 1/\eta_0)\langle \varphi_a^2 \rangle \\ &\quad + \frac{1}{2}(3 + \eta_0)(1 - 1/\eta_0)(\langle \varphi_c^2 \rangle + \chi)],\end{aligned}\quad (20)$$

where q_0 and η_0 refer to the rigid-lattice condition i.e., no motions of the NO_2^- group.

As regards the relaxation transition probabilities, one has to take into account, in principle, Eqs. (8) for the local contribution and Eq. (15) for the external contribution. Eq. (18), however, points out that the homogeneous (or $\vec{q} = 0$; see Sec. IID) dynamics in which the $s_i(t)$ take simultaneously the same value, does not induce effective modulation of the EFG from the external NO_2^- groups [Eq. (15)]. Since only for $q \approx 0$ enhancement and slowing down of the reorientational fluctuations are expected (as discussed below) we will disregard the contribution from Eq. (15) in

comparison to the one given by Eq. (8). Therefore Eqs. (2) will be written

$$W_+ = (\omega_+^0)^2 \int e^{-i\omega_+ t} g_1(t) dt = (\omega_+^0)^2 I_1(\omega_+), \quad (21a)$$

$$W_- = (\omega_-^0)^2 \int e^{-i\omega_- t} g_2(t) dt = (\omega_-^0)^2 I_2(\omega_-), \quad (21b)$$

$$W_d = (\omega_d^0)^2 \int e^{-i\omega_d t} g_3(t) dt = (\omega_d^0)^2 I_3(\omega_d), \quad (21c)$$

where

$$\omega_{\pm}^0 = \frac{3}{4} (e^2 q_0 Q / \hbar) (1 \pm \frac{1}{3} \eta_0)$$

and

$$\omega_d = \frac{1}{2} (e^2 q_0 Q / \hbar) \eta_0.$$

The correlation functions $g_i(t)$ are

$$g_1(t) \equiv \langle [\varphi_c(0) + f(0)][\varphi_c(t) + f(t)] \rangle, \quad (22a)$$

$$g_2(t) \equiv \langle \varphi_a(0) s(0) \varphi_a(t) s(t) \rangle, \quad (22b)$$

$$g_3(t) \equiv \langle \varphi_b(0) s(0) \varphi_b(t) s(t) \rangle. \quad (22c)$$

D. Transition probabilities and critical dynamics

To relate the transition probabilities [Eqs. (21)] to the critical reorientational dynamics the spectral densities I_i of the correlation function g_i must be evaluated.

By introducing collective order-disorder variables

$$s_{\vec{q}} = \frac{1}{\sqrt{N}} \sum_i s_i e^{i\vec{q} \cdot \vec{r}_i}, \quad (23)$$

a master equations mean-field (MFA) treatment¹⁵ allows us to write

$$\langle s_{\vec{q}}(0) s_{-\vec{q}}(t) \rangle = \langle |s_{\vec{q}}|^2 \rangle e^{-t/\tau_{\vec{q}}} \quad (24)$$

and

$$\langle |s_{\vec{q}}|^2 \rangle = kT \chi(\vec{q}, 0) = \tau_{\vec{q}} (1 - \langle s \rangle^2) / \tau_0. \quad (25)$$

The q -dependent relaxation time is $\tau_{\vec{q}} = \tau_0 / [1 - I(\vec{q})(1 - \langle s \rangle^2) / kT]$. τ_0 is the reorientational time of an individual NO_2^- dipole, in the absence of interactions. $I(\vec{q})$ is the Fourier transform of the dipole-dipole interaction.

For $\varphi_i(t)$ the classical equations for torsional harmonic oscillators will be used.¹⁶ For undamped oscillators, by taking into account Eqs. (9) and (24) in the random-phase approximation and by assuming no correlation between the value of φ^* and $s(t)$ one obtains

$$g_1(t) = \frac{1}{4} \langle \varphi^{*2} \rangle \frac{1}{N} \sum_{\vec{q}} (1 + \langle |s_{\vec{q}}|^2 \rangle) e^{-t/\tau_{\vec{q}}} \quad (26a)$$

[having omitted the deterministic contribution due to $\varphi_c(t)$] and

$$g_2(t) = \langle \varphi_a^2 \rangle \frac{1}{N} \sum_{\vec{q}} \langle |s_{\vec{q}}|^2 \rangle \cos \omega_a t e^{-t/\tau_{\vec{q}}}, \quad (26b)$$

$$g_3(t) = \langle \varphi_b^2 \rangle \frac{1}{N} \sum_{\vec{q}} \langle |s_{\vec{q}}|^2 \rangle \cos \omega_b t e^{-t/\tau_{\vec{q}}}. \quad (26c)$$

In deriving the above equations it has been taken into account that no abnormal dispersion along the branches causing the torsional oscillations is expected, in view of the lack of soft modes. Therefore, averaged frequencies ω_a and ω_b have been introduced, which should be close to the infrared and Raman resonance frequencies.¹⁷⁻¹⁹ From Eqs. (26), by considering that $\omega_{\pm, d} \tau_{\vec{q}} \ll 1$ and $\omega_{a, b} \tau_{\vec{q}} \gg 1$, one obtains

$$I_1(\omega_+) = \frac{1}{2} \langle \varphi^{*2} \rangle \frac{1}{N} \sum_{\vec{q}} (1 + \langle |s_{\vec{q}}|^2 \rangle) \tau_{\vec{q}}, \quad (27a)$$

$$I_2(\omega_-) = \frac{2}{N} \langle \varphi_a^2 \rangle \sum_{\vec{q}} \frac{\langle |s_{\vec{q}}|^2 \rangle}{\omega_a^2 \tau_{\vec{q}}}, \quad (27b)$$

$$I_3(\omega_d) = \frac{2}{N} \langle \varphi_b^2 \rangle \sum_{\vec{q}} \frac{\langle |s_{\vec{q}}|^2 \rangle}{\omega_b^2 \tau_{\vec{q}}}. \quad (27c)$$

In the presence of an appreciable damping of the torsional oscillatory modes the low-frequency spectral density for $\varphi_i(t)$ turns out to be a relaxational type with an effective relaxational time $\tau_e = 2\Gamma_i / \omega_i^2$ (Γ_i damping factor). For damping factors large enough that $\tau_{\vec{q}}^{-1} \ll \Gamma_i$, by noticing that $\sum_{\vec{q}} \langle |s_{\vec{q}}|^2 \rangle = N$, instead of Eqs. (27b) and (27c) one has

$$I_2(\omega_-) = 4 \langle \varphi_a^2 \rangle \Gamma_a / \omega_a^2, \quad (28b)$$

$$I_3(\omega_d) = 4 \langle \varphi_b^2 \rangle \Gamma_b / \omega_b^2, \quad (28c)$$

while I_1 [Eq. (27a)] is practically unchanged.

To perform the \vec{q} summation in Eqs. (27) we take into account the static and dynamical scalings²⁰ to write

$$\langle |s_{\vec{q}}|^2 \rangle = kT \chi(\vec{q}_c, 0) F(\vec{q}/\kappa), \quad (29a)$$

$$\tau_{\vec{q}}^{-1} = \tau_p^{-1} G(q/\kappa), \quad (29b)$$

where $\chi(\vec{q}_c, 0)$ is the reduced static dielectric susceptibility and τ_p is the relaxation time for the polarization fluctuations at the critical wave vector \vec{q}_c . F and G are homogeneous functions of q/κ only. κ is the inverse correlation length and $\kappa = \kappa_0 \epsilon^\nu$, $\epsilon = |T - T_0| / T_0$, ν being the corresponding critical exponent and T_0 the stability limit of the slowing down (for a second-order transition $T_0 = T_c$). For F and G we will assume

$$F(\vec{q}, \kappa) = G(\vec{q}, \kappa)^{-1} = \{1 + [(\vec{q} - \vec{q}_c)^2 + \delta^2 \cos^2 \theta] / \kappa^2\}^{-1}. \quad (30)$$

The above expression can deal with the deviation from the MFA, having added the term in $\cos^2 \theta$, (θ , angle between \vec{q} and the ferroelectric \vec{b} axis), related to the depolarizing effect of the dipole-

dipole interaction.²¹ This effect has been proven²² to play an important role in the temperature behavior of the relaxation rates.

By integrating, in Eqs. (27), over a Debye sphere according to Eqs. (29) and (30), W_+ becomes

$$W_+ = (\omega_+^0)^{2\frac{3}{8}} \pi \langle \varphi^{*2} \rangle kT \chi(\vec{q}_c, 0) \times \tau_p \epsilon^{\psi} (\kappa_0 \delta^{-1} \ln \epsilon^{-\nu} - 4/\pi), \quad (31)$$

where $q_0 \sim k_0$ has been set for the Debye wave vector. For negligible damping of the torsional oscillations (i.e., $\Gamma_i < \tau_i^{-1}$) one has, from Eqs. (27b) and (27c),

$$W_- = (\omega_-^0)^2 (2 \langle \varphi_a^2 \rangle / \omega_a^2) (kT / \tau_p) \chi(\vec{q}_c, 0), \quad (32a)$$

$$W_d = (\omega_d^0)^2 (2 \langle \varphi_b^2 \rangle / \omega_b^2) (kT / \tau_p) \chi(\vec{q}_c, 0), \quad (32b)$$

while, in the presence of sizeable damping, from Eqs. (28),

$$W_- = (\omega_-^0)^2 4 \langle \varphi_a^2 \rangle \Gamma_a / \omega_a^2, \quad (33a)$$

$$W_d = (\omega_d^0)^2 4 \langle \varphi_b^2 \rangle \Gamma_b / \omega_b^2. \quad (33b)$$

For $T < T_c$, where $\langle s \rangle \neq 0$, Eqs. (32a) and (32b) can still be used by simply multiplying them by $(1 - \langle s \rangle^2)$. Equation (31) can be used in the ordered phase, simply by dividing it by $(1 - \langle s \rangle^2)$, only in the temperature range in which the reorientational fluctuations are still fast, i.e., $\omega_+ \tau_i \ll 1$. For slow fluctuations a more complicated expression should be considered. In addition, when $\omega_+ \tau_0 \lesssim 1$ a completely different relaxation mechanism can occur.²³ We will not consider these effects here.

Since

$$kT \chi(\vec{q}_c, 0) = \epsilon^{-\gamma}, \quad (34a)$$

$$\tau_p = \tau_0 \epsilon^{-\Delta}, \quad (34b)$$

in the MFA, where $\Delta = \gamma = 2\nu = 1$, only a logarithmic divergence in W_+ should be expected on approaching T_c . The temperature dependence of W_- and W_d should be driven by noncritical quantities, even if negligible damping is assumed.

Finally, it can be noted that for $\varphi^* = 0$ in Eq. (3), i.e., reversal of the Ising variable by an exactly π angle, no critical effects would occur in the relaxation rates [as well as in the quadrupole frequencies, according to Eqs. (19) and (20)].

III. EXPERIMENTAL RESULTS

A. Experimentals

The ^{14}N NQR measurements in NaNO_2 were performed by means of a Matec Inc. pulse spectrometer. A HP2114B computer operated on line, accumulating and processing the signals.

The piezoelectric resonances were suppressed by finely grinding the NaNO_2 crystals. The sam-

ple was located in Haake thermostat. Up to 180°C low-viscosity Vaseline oil was used as a thermostatic liquid, allowing fast flowing. Practically no detectable temperature gradients around the sample were observed. For temperatures greater than about 180°C silicon oil was used. The long-term stability was about 10⁻²°C. The temperature was measured by means of a standardized Pt resistance, with resolution around 10⁻²°C. Precise evaluation of the quadrupole resonance frequencies and linewidths were obtained as follows. The free-induction decay (FID) signals, phase detected slightly off resonance, were accumulated and then Fourier transformed on a spectral range of 20 kHz, with 256 data points per pulse. In the antiferroelectric phase (164.8 ≤ T ≤ 166°C) sizeable signals could be obtained only by accumulating up to 10⁴ FIDs. The Fourier transformation was essential to put in evidence, in the above temperature range, the splitting of the ν_+ and ν_- lines in two components (see below).

The quadrupole relaxation measurements were usually performed by the (90°-t-90°)_n pulse sequence and around the transition also by the repeating 90° pulse method.^{23,24} In the antiferroelectric phase the strong decrease of the signal-to-noise ratio inhibits reliable relaxation measurements in view of the too long accumulation time necessary for a complete measurement.

B. Quadrupole resonance frequencies and linewidths

In Fig. 1 the ^{14}N NQR frequencies ν_+ and ν_- around the transitions are reported. From the ν_+ line the transition temperature from the paraelectric to the antiferroelectric phase results $T_c^A = 166.0 \pm 0.04$ °C; for the transition from the antiferroelectric to the ferroelectric phase T_c^F

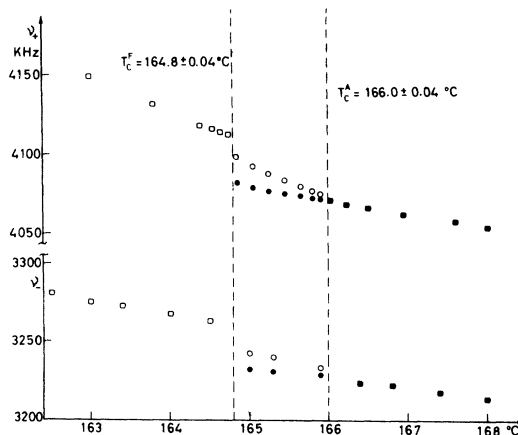


FIG. 1. ^{14}N NQR frequencies ν_+ and ν_- in NaNO_2 around the ferro- and antiferroelectric transitions.

$= 164.8 \pm 0.04^\circ\text{C}$.

In the paraelectric phase, up to about 220°C (data not reported in the figure) ν_+ and ν_- vs T is well fitted by a straight line, with temperature coefficients $7.2\text{ kHz}/^\circ\text{K}$ and $5.4\text{ kHz}/^\circ\text{K}$, respectively. In the ordered phases the ν_+ frequencies are characterized by a more complex temperature behavior, which can be related to the raising of the order parameter $\langle s \rangle$, as will be discussed in Sec. IV.

In the antiferroelectric phase the Fourier-transformed FIDs clearly evidence the splitting of both the ν_+ and ν_- lines into two components (see Fig. 2) for the ν_+ . The resonance frequencies of these components show the temperature dependence reported in Fig. 1. The lines at higher frequencies (corresponding to the "feeble" ones in the spectra reported in Fig. 2) show a temperature behavior as in the ferroelectric phase. The lines at lower frequencies ("strong" lines in Fig. 2) show a temperature behavior as in the paraelectric phase.

From the transformed FIDs the linewidth $\delta\nu$ at half intensity of the resonance lines was evaluated. The results are shown in Fig. 3. In the antiferroelectric phase the wider line is that with the ferroelectric-type temperature dependence. As appears from the figure, on approaching the transitions only a small increase of the linewidth occurs. The linewidths around the transitions are consistent with the values of T_2^* reported by Petersen and Bray,¹² for a Lorentzian line shape ($\delta\nu = 1/\pi T_2^*$).

C. Effective relaxation rates

The spin-spin couplings are unable to establish a spin temperature and for $\eta \neq 0$ a definition of the spin-lattice relaxation time T_1 is not trivial. In a master equation approach the recovery laws

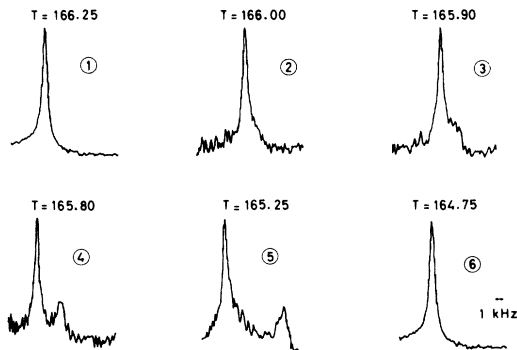


FIG. 2. Fourier transform of some ν_+ line FIDs around the transitions, obtained by accumulating 10^4 signals. The splitting of the line, as well as the decreasing of the signal-to-noise ratio in the antiferroelectric phase, can be observed.

for the populations can be easily obtained.²⁴ A nonexponential recovery occurs, the time constants and the coefficients of the two exponentials depending on the method (double 90° pulse, repeating 90° pulse, saturating comb and 90° pulse) used to measure the relaxation.

Precise evaluations of the time constants as well as of the coefficients are difficult to achieve from a nonexponential recovery plot. In fact, the full estimate requires the analysis of the recovery plot also at long times and nonphysical results for the transition probabilities can be obtained.¹² As already observed by Vega,²⁵ it is often convenient, particularly in powder, to define an effective relaxation rate $(T_1)_e^{-1}$ as the slope of the tangent at the origin of the semilogarithmic recovery plot $\ln\{[s(\infty) - s(t)]/s(\infty)\}$ vs t . From the master equations for the level populations, with the principle of the detailed balance, $(T_1)_e^{-1}$ can be obtained by a straightforward procedure. The following results were obtained:

(i) Double 90° pulse method:

$$(T_1)_{e,+}^{-1} = 2W_+ + \frac{1}{2}(W_- + W_d) \quad (35a)$$

for detection of the ν_+ line;

$$(T_1)_{e,-}^{-1} = 2W_- + \frac{1}{2}(W_+ + W_d) \quad (35b)$$

for detection of the ν_- line.

(ii) Repeated 90° pulse method:

$$(T_1)_{e,+}^{-1} = 2(2W_+W_- + 2W_+W_d + W_dW_- - W_+^2 - W_-^2 - W_d^2)/(W_- + W_d) \quad (36)$$

for detection of the ν_+ line; for the ν_- line the denominator in the above equation is $(W_+ + W_d)$. For the method of the saturating comb¹² Eqs. (35) hold.

At high temperatures both the recovery of the ν_+ and ν_- signals were observed to be dominated by a single exponential. In this case, the time con-

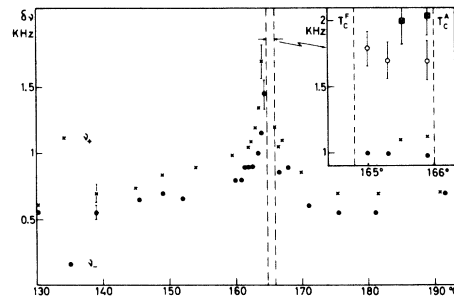


FIG. 3. Linewidths (at half intensity) of the Fourier-transformed FIDs for the ν_+ lines and the ν_- lines. In the enlarged part of the figure some representative results in the antiferroelectric phase, for both the two ν_+ and the two ν_- components, are reported (see the text).

stant is close to $(T_1)_e$ as defined in Eqs. (35) and (36).

In Fig. 4 the effective relaxation rates $(T_1)_e^{-1}$ for the ν_+ and ν_- lines are reported.

IV. DISCUSSION AND CONCLUSIONS

From Eqs. (19) and (20) the theoretical temperature dependence of the quadrupole resonance frequencies results:

$$\nu_{\pm} = \frac{3}{4} (e^2 Q q_0 / \hbar) \left[1 - \frac{1}{2} (3 + \eta_0) (1 \pm \frac{1}{3}) (\langle \varphi_c^2 \rangle + \chi) - \frac{1}{2} (3 - \eta_0) (1 \mp \frac{1}{3}) (\langle \varphi_a^2 \rangle \pm \frac{1}{3} \eta_0 (1 - 2 \langle \varphi_b^2 \rangle)) \right]. \quad (37)$$

By considering that for a torsional harmonic oscillator

$$\langle \varphi_i^2 \rangle = \frac{\hbar}{I_i \omega_i} \left(\frac{1}{2} + \frac{1}{\exp(\hbar \omega_i / kT) - 1} \right), \quad (38)$$

(where I_i are the moments of inertia) and by taking into account the results by Raman spectroscopy¹⁹ for ω_a , ω_b , and ω_c (mode assignment B_1 , A_2 , and

$$\frac{d\nu_{\pm}}{dT} \approx -\frac{3}{4} \left(\frac{e^2 Q q_0}{\hbar} \right) k \left(\frac{3 + \eta_0}{2} (1 + \frac{1}{2} a) (1 \pm \frac{1}{3}) \frac{1}{I_c \omega_c^2} + \frac{3 - \eta_0}{2} (1 \mp \frac{1}{3}) \frac{1}{I_a \omega_a^2} \pm \frac{2\eta_0}{3} \frac{1}{I_b \omega_b^2} \right). \quad (39)$$

The rotational frequencies are of the same order of magnitude, while $I_c \approx 7 \times 10^{-40}$, $I_a \approx 65 \times 10^{-40}$, and $I_b \approx 58 \times 10^{-40}$ g cm². Therefore the first term in the second large parentheses in Eq. (39) should be dominant and negative temperature coefficients with $|d\nu_+/dT|$ greater than $|d\nu_-/dT|$ by a factor of almost 2 should be expected.

In the antiferro- and ferroelectric phases, besides the noncritical Bayer-type contributions due to $\langle \varphi_i^2 \rangle$, an extracontribution Δ_{\pm} to the quadrupole frequencies is present, related to the critical ordering of the dipoles. From Eq. (37)

$$\Delta_{\pm} = \frac{3}{16} (3 + \eta_0) (e^2 Q q_0 / \hbar) (1 \pm \frac{1}{3}) \langle \varphi^{*2} \rangle \langle s \rangle. \quad (40)$$

Quantitative comparisons require the knowledge of the rigid-lattice NQR parameters and the average rotational frequencies. In Fig. 5 we report the theoretical plots for $\Delta_{\pm}(T)$ and for $\nu_{\pm}(T)$ according to Eqs. (40) and (37). $e^2 Q q_0 / \hbar$ and η_0 have been obtained by extrapolating the resonance frequencies¹² at zero temperature; for the rotational frequencies we have used¹⁹ $\omega_a \approx 130$ cm⁻¹, $\omega_b \approx 110$ cm⁻¹, and $\omega_c \approx 220$ cm⁻¹ (by neglecting their temperature dependence). For the order parameter $\langle s \rangle$ the results from spontaneous polarization measurements²⁶ have been used; for a in Eq. (4) we set $a = 1$. As appears from the comparison with the experimental results a good agreement is obtained. In particular, it can be observed that the anomalous fast decreasing of the quadrupole frequencies on approaching T_c in the ferroelectric

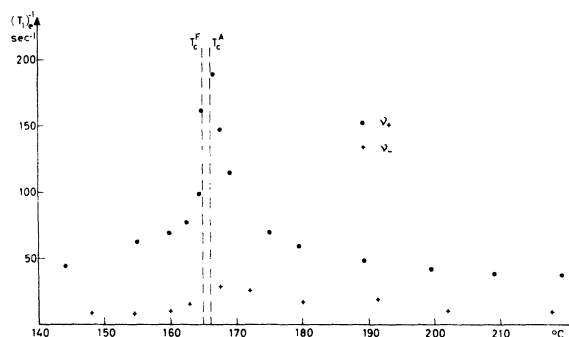


FIG. 4. Effective ¹⁴N relaxation rates $(T_1)_{e,\pm}^{-1} = 2W_{\pm} + \frac{1}{2}(W_{\pm} + W_d)$ in NaNO₂ for the ν_+ (●) and ν_- (▲) lines, vs T .

B_2 , respectively), Eq. (37) satisfactorily explains the temperature behavior of ν_+ and ν_- . In the paraelectric phase, where $\chi = \frac{1}{2} \langle \varphi^{*2} \rangle = \frac{1}{2} a \langle \varphi_c^2 \rangle$, from Eqs. (37) and (38) one obtains

phase (already noted by other authors^{8,9,11,27}) is thus justified by the theoretical picture developed in Sec. III, only by taking into account the critical reorientation of the dipoles. It does not seem necessary to postulate a crystal deformation linearly depending on the spontaneous polarization²⁸ and/or an anomalous increase in the amplitude of the torsional oscillations (at least in a first approximation and close to the transition).

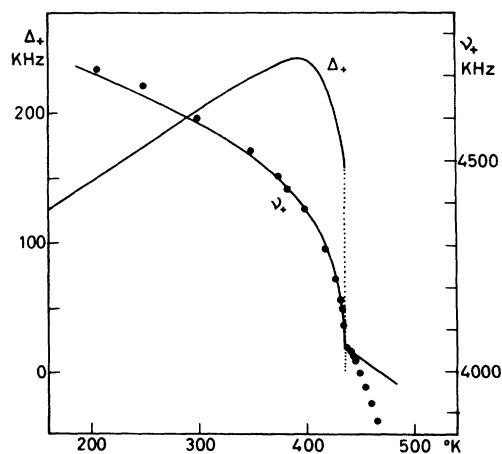


FIG. 5. Theoretical plots of the extracontribution $\Delta_{\pm}(T)$ to the ν_{\pm} NQR frequency in the ferroelectric phase [according to Eq. (40) in the text] and of $\nu_{\pm}(T)$ [Eq. (37)]. Some representative experimental data for ν_+ are reported for the comparison.

In the antiferroelectric phase, in the light of Eq. (40), the two components of the ν_+ and ν_- lines (Fig. 1) can be attributed to nuclei having $\langle s \rangle = 0$ and $\langle s \rangle \neq 0$. By taking into account also the linewidths (Fig. 3), the components at higher frequency should pertain to short-range ordered domains, where a ferroelectric-type ordering is present. The low-frequency components should be attributed to regions at the boundaries of those domains, where the order parameter is practically zero. From the relative magnitudes of the components it appears that only about (30–40)% of the nuclei are inside the short-range ordered domains of ferroelectric type. This consideration supports the early observation by Yamada *et al.*²⁹ based on the temperature dependence of the x-ray diffraction intensities. A completely regular antiphase structure can be disregarded, in favor of a smooth modulation of the order parameter along the a axis. Finally, from Fig. 1, the second-order character of the transition from the paraelectric to the antiferroelectric phase is put in evidence, while the transition to the ferroelectric phase appears slightly first order, with a small discontinuity in $\langle s \rangle$. According to our estimates, in the light of Eqs. (40) and (38) the discontinuity in $\langle s \rangle$ at T_c^F should be around 5×10^{-2} .

In the paraelectric phase, Fig. 5 puts in evidence that the temperature coefficient of ν_+ is greater than the one theoretically evaluated by using the same values for the various parameters (q_0 , η_0 , ω_i , and a) as in the ferroelectric phase. This should not prove, by itself, the existence of a short-range order in the paraelectric phase. In this case, in fact, no discontinuity at T_c^F would be expected and a very broad line should be observed in the paraelectric phase (in contrast to the experimental results). The large temperature coefficient of the resonance frequency for $T \geq 460$ °K may be due to a marked increase in the amplitude of the torsional oscillations of the NO_2^- group, possibly also related to approaching the melting temperature (≈ 550 °K).

Let us now briefly discuss the NQR parameters in connection with the critical dynamics. As shown in Fig. 3 the linewidths $\delta\nu$ increase on approaching the transitions. The NQR linewidth should be given¹³ by an adiabatic term related to spectral densities at zero frequency and a second term related to the lifetime of the levels. Therefore, the increase in $\delta\nu$ should be attributed to the same process causing the increase in the relaxation rates. The information on the critical dynamics can then be obtained directly by analyzing $(T_1)_e^{-1}$ in Fig. 4. The ratio of the relaxation rates for the ν_+ and ν_- lines far from T_c is around four. In the light of Eqs. (36) this means that W_+ is greater

than W_- and W_d .

Order-of-magnitude estimates support this consideration. From Eq. (32a), by using the MFA condition of thermodynamical slowing down¹⁵ $\chi(\vec{q}_c, 0)/\tau_p = \chi_0/\tau_0$ and by taking into account Eq. (38) one obtains

$$W_- \approx 2(\omega_-^0)^2 kT / I_a \omega_a^4 \tau_0.$$

For $\tau_0 \approx 10^{-11}$ sec,³ and $\omega_a \approx 130$ cm⁻¹, $W_- \approx 3 \times 10^{-3}$ sec⁻¹. If the damping is taken into account, by using the linewidth of the Raman resonance¹⁹ at about 180 °C for Γ_a , one has, from Eq. (33a),

$$W_- \approx 4(\omega_-^0)^2 kT \Gamma_a / I_a \omega_a^4 \approx 0.45 \text{ sec}^{-1}.$$

The above value appears of the correct order of magnitude and seems to put in evidence the relevance of the damping of the rotational modes. From Eqs. (33), the ratio

$$\frac{W_-}{W_d} = \left(\frac{3 - \eta_0}{2\eta_0} \right)^2 \frac{\langle \varphi_a^2 \rangle \omega_b^2 \Gamma_a}{\langle \varphi_b^2 \rangle \omega_a^2 \Gamma_b}$$

should be of some units, according to the Raman and infrared data.¹⁷⁻¹⁹ Regarding W_+ , by taking into account the dielectric measurements for τ_0 and for T_0 ($T_0 = T_c^F - 1.27$), and by setting $\gamma = \Delta = 2\nu = 1$ and $k_0 \sim \delta$ one obtains, from Eqs. (31) and (34), at $T \approx 180$ °C,

$$W_+ \approx (\omega_+^0)^2 3\pi a \langle \varphi_c^2 \rangle \tau_0^{\frac{1}{8}} (\ln \epsilon^{-1/2} - 4/\pi) \\ \approx 230 \text{ sec}^{-1} \text{ for } a = 1,$$

very much greater than W_- and W_d , as expected.

Regarding the temperature dependence of the relaxation rates, we will only discuss the behavior of $(T_{1e^+})^{-1} \approx 2W_+$ in the paraelectric phase. According to Eqs. (31) and (34) one has

$$(T_{1e^+})^{-1} \propto -T\tau_0 \epsilon^{-(\Delta-\gamma)} \ln \epsilon + \text{const.} \quad (41)$$

In Fig. 6 the experimental results for $(T_{1e^+})^{-1}$ are reported versus $\ln \epsilon$ and compared with the theoretical behaviors for some values of $\Delta - \gamma = \phi$. The logarithmic divergence seems to explain the results for $\epsilon \geq 10^{-2}$ ($T \approx 171.5$ °C) while for lower temperatures the experimental results indicate $\Delta \neq \gamma$. A satisfactory fitting is obtained for $\phi \approx +0.1$. Some evidence of the breakdown of the thermodynamical slowing-down condition $\Delta = \gamma$ was already obtained by Hatta,³ from the analysis of the dielectric measurements, with a maximum value for ϕ of 0.2.

In conclusion, a kinematical Ising model for the critical reversal of the NO_2^- dipoles, superimposed on the ordinary torsional oscillator dynamics, appears to describe satisfactorily the temperature behavior of the ¹⁴N NQR parameters around the ferro and antiferroelectric transitions in NaNO_2 . A crucial role is played by the angle ϕ^* which measures the departure of the reversal

of the dichotomic variable $s(t)$ by an angle π . For $\phi^* = 0$ no effect on the quadrupole frequencies, the linewidths and the relaxation rates would occur. A small ϕ^* , of the order or less than the mean-square angle of the torsional oscillations around the \vec{c} axis, consistently explains the experimental results.

Experimentally, accurate measurements based on pulsed technique and Fourier transformation of the ^{14}N free-induction decay allowed us to detect, for the first time, the ^{14}N NQR signals in the antiferroelectric phase. A splitting in two components of both the ν_+ and ν_- lines was observed. The two components were attributed to nuclei inside short-range ordered domains with $\langle s \rangle \neq 0$ and to nuclei at the boundaries of these domains, with $\langle s \rangle \approx 0$.

From the analysis of the experimental results in the light of the theoretical picture interesting information on the phase transitions and the critical dynamics were obtained. The transition from the paraelectric to the antiferroelectric phase appears to be second-order type. The transition towards the ferroelectric phase, instead, is confirmed to be slightly first order, with a small discontinuity in the order parameter.

In the ferroelectric phase the temperature dependence of the quadrupole frequencies can be explained by taking into account, besides the torsional oscillations of the NO_2^- group, the temperature dependence of the order parameter. The ^{14}N NQR relaxation appears to be dominated by the fluctuations of the EFG component V_{yz} (with $\vec{y} \parallel \vec{a}$ and $\vec{z} \parallel \vec{b}$), due to the critical reversal of $s(t)$ and to the torsional oscillations around the \vec{c} axis. The enhancement and the slowing down of the reorientation fluctuations of approaching T_c cause a divergence of the relaxation rates close to a logarithmic type, consistent with the dipolar character of the interactions driving the phase transitions. Close to T_c some evidence of a breakdown of the thermodynamical slowing down (critical index for the susceptibility different from that for

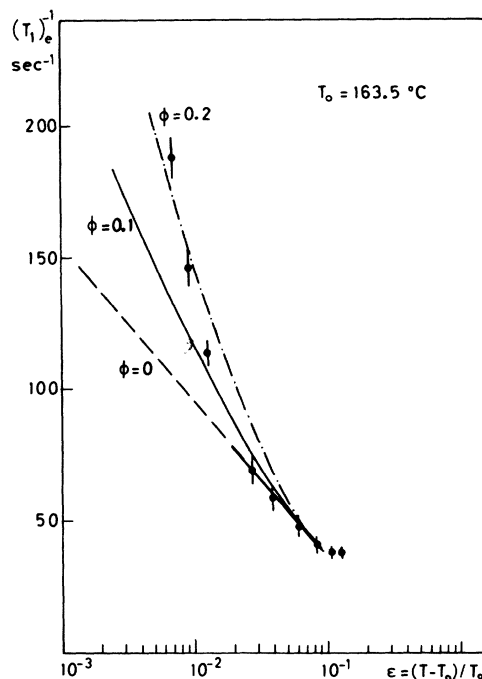


FIG. 6. Semilogarithmic plot of $(T_1)_e^{-1}$ for the ν_+ line vs the reduced temperature ϵ compared with the theoretical behaviors [Eq. (41) in the text] for different values of $\phi = \Delta - \gamma$. For τ_0 the temperature behavior $\tau_0 \propto T^{-1} \exp(2368/T)$ was used (see Ref. 3).

the relaxation time of the polarization fluctuations) is obtained.

ACKNOWLEDGMENTS

The authors wish to thank G. Petersen for sending his thesis before the publication of the results. One of us (A.R.) is also indebted to R. Blinc for a useful discussion and to R. De Micheli for the helpful collaboration in bringing out some points in the theory. A discussion of the paper with J. L. Bjorkstam is gratefully acknowledged.

¹For a short review of various experiments on the microscopic mechanism of the NO_2^- fluctuations as well as their coupling with lattice phonon modes, see: M. I. Kay, J. A. Gonzalo, and R. Maglic, *Ferroelectrics* **9**, 179 (1975).

²I. Hatta, T. Sakudo, and S. Sawada, *J. Phys. Soc. Jpn.* **21**, 2162 (1966).

³I. Hatta, *J. Phys. Soc. Jpn.* **28**, 1266 (1970).

⁴I. Hatta, *J. Phys. Soc. Jpn.* **38**, 1430 (1975).

⁵J. Sakurai, R. A. Cowley, and G. Dolling, *J. Phys. Soc. Jpn.* **28**, 1426 (1970).

⁶A. S. Barker, Jr., *Phys. Rev. B* **12**, 4071 (1975).

⁷H. Beck, *J. Phys. C* **9**, 33 (1976).

⁸T. Oja, R. A. Marino, and P. J. Bray, *Phys. Lett. A* **26**, 11 (1967).

⁹P. K. Kadaba, D. E. O'Reilly, and R. Blinc, *Phys. Status Solidi* **42**, 855 (1970).

¹⁰Y. Abe, Y. Ohneda, S. Abe, and S. Kojima, *J. Phys. Soc. Jpn.* **33**, 864 (1972).

¹¹S. Singh and K. Singh, *J. Phys. Soc. Jpn.* **36**, 1588 (1974).

¹²G. L. Petersen and P. J. Bray, *J. Chem. Phys.* **64**, 522 (1976).

¹³See A. Abragam, *The Principles of Nuclear Magne-*

tism (Oxford University, London, 1961), Chap. X, Sec. VI.

¹⁴R. A. Marino and P. J. Bray, *J. Chem. Phys.* **48**, 4833 (1968); see also R. A. Marino, Ph.D. thesis (Brown University, 1969) (unpublished).

¹⁵See K. Kawasaki, in *Phase Transitions and Critical Phenomena*, edited by C. Domb and M. S. Green (Academic, New York, 1972).

¹⁶A quantum-mechanical evaluation of the correlation function for a torsional harmonic oscillator has been given [D. E. Woessner and H. S. Gutowsky, *J. Chem. Phys.* **39**, 440 (1963)]. To check the reliability of a classical approach the following comparison can be made. For fast motions, the spectral density at low frequencies for the quantum-mechanical torsional oscillator coincides with that for the classical damped oscillator (i.e., $2\langle\varphi^2\rangle\tau_{\text{eff}}$, where $\langle\varphi^2\rangle = kT/I\omega_0^2$ and $\tau_{\text{eff}} \approx 2\Gamma/\omega_0^2 \sim \omega_0^{-1}$, Γ being the damping factor, ω_0 and I the appropriate classical rotational frequency and moment of inertia) if $\Lambda = (\hbar/\tau_a) \coth(\hbar\omega/2kT)$ is equal to kT .

$$\tau_a^{-1} = \sum_{r=0}^{\infty} f_r \tau_r^{-1}$$

and f_r is the relative population in the r th rotational level and τ_r the average lifetime in the level. For a crude order-of-magnitude estimate pertaining to the NO_2^- group in NaNO_2 , one can assume τ_a^{-1} of the order of the frequencies evaluated by infrared and Raman spectroscopies (see Refs. 17–19). For T around

400°K, Λ results kT times a constant around 1.8–2.

Therefore a classical approach for the correlation function for the torsional oscillations of the NO_2^- groups in NaNO_2 around the transition appears acceptable.

¹⁷M. K. Barnoski and J. M. Ballentine, *Phys. Rev.* **174**, 946 (1968).

¹⁸E. V. Chisler and M. S. Shur, *Phys. Status Solidi* **17**, 163 (1966).

¹⁹C. M. Hartwig, E. Wiener-Avneer, and S. P. S. Porto, *Phys. Rev. B* **5**, 79 (1972).

²⁰See H. E. Stanley, *Introduction to Phase Transitions and Critical Phenomena* (Clarendon, Oxford, 1971).

²¹I. Tatsuzaki, K. Sakata, I. Todo, and M. Tokunaga, *J. Phys. Soc. Jpn.* **33**, 438 (1972).

²²G. Bonera, F. Borsa, and A. Rigamonti, *Phys. Rev. B* **2**, 2784 (1970). See also various contributions in

Local Properties at Phase Transitions, edited by K. A. Müller and A. Rigamonti (North-Holland, Amsterdam, 1976).

²³S. Alexander and A. Tzalmona, *Phys. Rev.* **138**, A845 (1965).

²⁴Y. Abe, Y. Ohneda, M. Hirota, and S. Kojima, *J. Phys. Soc. Jpn.* **37**, 1061 (1974).

²⁵S. Vega, *J. Chem. Phys.* **61**, 1093 (1974).

²⁶K. Hamano, 25th Meeting of the Physical Society of Japan, Tokyo (1970) (unpublished); see also T. Yagi and I. Tatsuzaki, *J. Phys. Soc. Jpn.* **32**, 750 (1972).

²⁷H. Betsuyaku, *J. Phys. Soc. Jpn.* **27**, 1485 (1969).

²⁸J. Stankowski, *Phys. Status Solidi* **34**, K173 (1969).

²⁹Y. Yamada, I. Shibuya, and S. Hoshino, *J. Phys. Soc. Jpn.* **18**, 1594 (1963).